Acid-Resistant Catalysis without Use of Noble Metals: Carbon Nitride with Underlying Nickel

Teng Fu,[†] Meng Wang,[†] Weimeng Cai,[†] Yuming Cui,[†] Fei Gao,[†] Luming Peng,[†] Wei Chen,[‡] and Weiping Ding*,[†]

[†]Key Lab of Mesoscopic Chemistry, School of Chemistry and Chemical Engineering, Nanjing University, Nanjing 210093, China
[‡]Department of Chemistry, National University of Singapore, 3 Science Drive 3, Singapore 117543, Singapore

S *Supporting Information*

ABSTRACT: A nanocomposite able to function as a hydrogenation catalyst under strongly acidic conditions without the presence of noble metals is synthesized and thoroughly studied. This specially designed catalyst possesses a unique structure composed of carbon nitride (CN) with underlying nickel, in which the nickel endows the CN with new active sites for hydrogen adsorption and activation while it itself is physically isolated from the reactive environment and protected from poisoning or loss. The CN is inert for hydrogenation without the help of nickel. The catalyst shows good performance for hydrogenation of nitro compounds under strong acidic conditions, including the one-step hydrogenation of nitrobenzene in 1.5 M H_2SO_4 to produce *p*-amoniophenol, for which the acid in the reaction system has restricted the catalyst only to noble metals in previous studies. Further characterization has demonstrated that the nickel in the catalyst is in an electron-deficient state because some of its electron has been donated to CN (HRTEM, PES); thus, the hydrogen can be directly adsorbed and activated by the CN (HD exchange, in situ IR and NMR). With this structure, the active nickel is protected by inert CN from the corrosion of acid, and the inert CN is activated by the nickel for catalytic hydrogenation. The assembly of them gives a new catalyst that is effective and stable for hydrogenation even under a strongly acidic environment.

KEYWORDS: hydrogenation, corrosion-resistance, carbon nitride, hetero junction, noble metal free
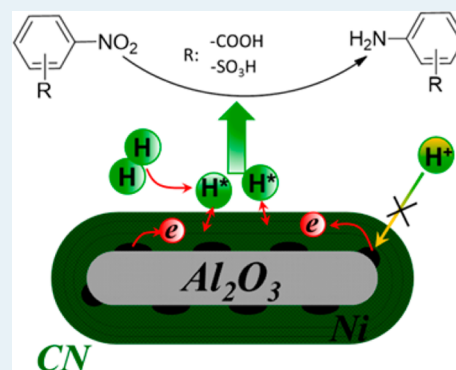
1. INTRODUCTION

Among the numerous catalytic hydrogenation reactions, some need to proceed under acidic conditions or with sulfur existence in the reaction system, such as the hydrogenation of $-NO_2$ in the molecules, as shown in Scheme 1. The catalysts used in these reactions should be acid- and sulfur-resistant. Under these conditions, commonly, nickel is inactive and noble metals such as Pt or Pd are active but would suffer from poisoning and loss in such a reaction. From the perspective of green chemistry and sustainable development, the traditional method by neutralizing the acidic compound with subsequent acidification should be avoided, and it is important to find an alternate to replace the noble metal that could function under acidic conditions for which its large-scale application has been limited by high costs. This has raised challenge to the synthesis of corresponding catalysts that are able to function under such harsh conditions.

In traditional hydrogenation processes, such as A or B in Scheme 1, the acid of the reactants is often neutralized by bases and followed by iron-acid reduction steps or catalytic hydrogenation, and then products are recovered by acidification, resulting in an extremely low total atomic efficiency of the reaction. Moreover, for the direct hydrogenation of nitrobenzene to *p*-amoniophenol (C in Scheme 1), the reaction starts with a partial hydrogenation to produce phenylhydroxyl amine and is followed by an in situ acid-catalyzed Bamberger rearrangement to *p*-amoniophenol. Because the reaction could

Scheme 1[a]
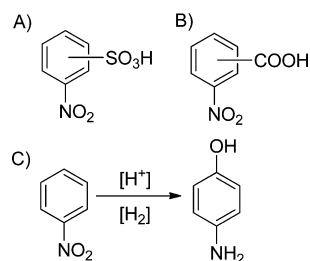
[a](A, B) Some acidic molecules with $-NO_2$ hydrogenation needed to produce more important molecules. (C) The hydrogenation and simultaneous isomerization must happen under strongly acidic conditions for the synthes is of *p*-amoniophenol from nitrobenzene in one-step hydrogenation.

be conducted only under strongly acidic conditions, noble metal catalysts are almost the only choice (Pt or Pd);[1−5] however, the serious loss of noble metals makes the process uneconomical for large-scale applications. It is necessary to develop a catalyst with new concepts that could effectively work under the harsh conditions. We have demonstrated in this investigation that the CN material with a suitable underlying metal is promising as a candidate for the processes.

Carbon nitride (CN) with a structural inscape of covalently sp^2 bonded atoms of carbon and nitrogen has unique and versatile properties.[6−12] Its electronic state is very sensitive to the materials it contacts,[13,14] and the electron could be donated to the CN, or vice versa. As a catalyst, CN itself has shown interesting properties in photocatalyzing water splitting, oxygen reduction, and some heterogeneous reactions[15−20] because of its unique electronic and structural properties. For exaple, its densities of state at the Fermi level increase linearly with the increasing nitrogen content and form a metal-like material.[21,22] With surface defects and nitrogen atoms for both electron localization and anchoring the active site, CN material has become a competitive candidate to support metal nano-particles.[12,23−27] The metal−CN heterojunction has been proved to improve photocatalytic hydrogen evolution under visible light.[28] All the results suggest that some metals have strong interactions with the CN material when physical contact between them is established, which makes it possible to modify the properties of CN, although the CN itself is rather inert under common acidic or basic conditions. Considering the demand for catalytic hydrogenation under harsh conditions, we have designed a unique structure with nickel-underlying CN to form a strong interaction between them and to provide active sites to CN for hydrogen adsorption and activation while the nickel itself is physically isolated from the reactive environment and protected from poisoning or loss.

2. RESULT AND DISCUSSION

Experimentally, highly dispersed nickel was first deposited on Al_2O_3 by the impregnation method. The NiO/Al_2O_3 was then encapsulated with carbon nitride via a solution synthesis. Using a method similar to that reported by Gao et al, ethylenediamine and tetrachloride were used as precursors for the deposition of well-structured layered carbon nitride.[29] The sample was further heated to form the encapsulated structure of $CN/Ni/Al_2O_3$ at 873 K in Ar. During the heat treatment, the organic precursors carbonized to CN and, at the same time, the NiO dispersed on alumina was reduced to metallic nickel (also see the Supporting Information (SI)).

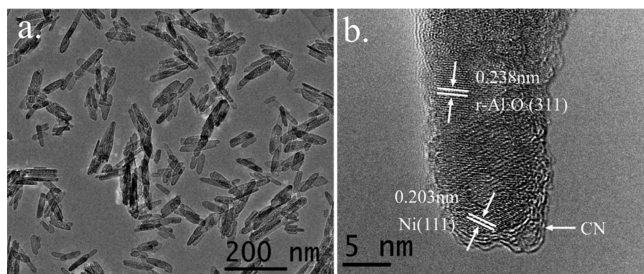Figure 1a shows the morphology of the Al_2O_3 possessing a uniform rodlike structure with diameters of 10−20 nm. With the encapsulation by CN, the HRTEM image of $CN/Ni/Al_2O_3$ after heating in N_2 gives rise to the special structure of the catalyst, as shown in Figure 1b. The appearance of the (111) planes of nickel reveals that the nickel is reduced to its metallic state during the formation of the CN at high temperature. After the formation of CN is completed, the CN encapsulates the nickel to prevent its being oxidized. This is different from the previous report in which the transition metals were incorporated into graphitic C_3N_4 in their oxidation state[30] or loaded onto the surface. The layered CN surrounding the surface of the catalyst particle is in a thickness of several layers. All the samples show the characteristic XRD peaks indexed to γ-alumina, and no new peak can be observed; thus, the formation of $NiAl_2O_4$ could be excluded (SI Figure S1). Because the XRD patterns of CN/Al_2O_3 and $CN/Ni/Al_2O_3$ did not show the typical (002) peak of CN, IR was conducted to verify the formation of CN. Both the IR spectra of CN/Al_2O_3 and $CN/Ni/Al_2O_3$ show similar characteristic absorptions (C−N stretching modes between 1120 and 1620 cm^{-1}, N−H stretching vibration around 344 cm^{-1}) ascribed to CN (SI Figure S2).[29] In addition, the XPS analysis shows the typical binding energy of carbon and nitrogen in CN (Figure 2). Before heat treatment, the TEM (not shown) and XRD (SI Figure S1) were unable to detect NiO in the sample NiO/Al_2O_3, implying the high dispersion of NiO on the surface of Al_2O_3.

The amount of CN in $CN/Ni/Al_2O_3$ and CN/Al_2O_3 has been analyzed by thermogravimetric analysis (TG) as 20 and 22 wt %, respectively (SI Figure S2, inset). Considering the amount of CN and the surface area of the alumina used, the thickness of CN can be calculated as 3−4 layers covering the catalyst particles, in agreement with the TEM observation. It suggests that by this synthetic process, we can obtain a material with a controlled amount of CN encapsulating nickel-loaded alumina, or the CN with underlying metallic nickel.

The catalytic results of hydrogenation of p-nitrobenzoic acid at different pH values are listed in Table 1. Entries 1 and 2 provide the catalytic results of Ni/Al_2O_3. As the pH value decreases from 3.6 to ∼2, almost no conversion of p-nitrobenzoic is detected, indicating that the concentrated proton would adsorb and hinder the adsorption and activation of H_2 on the surface of nickel during the reaction. This makes the catalyst inactive under the acidic condition. Moreover, the nickel would gradually dissolve under the acidic condition.

In contrast, $CN/Ni/Al_2O_3$ possesses good activities under the acidic conditions, as listed in entries 5, 6, and 7. Even at a pH value of 1.0 resulting from adding sulfuric acid, the catalyst still shows fairly good catalytic performance for the hydro-genation of the p-nitrobenzoic acid. To further test the robustness of $CN/Ni/Al_2O_3$, the etching experiments were carried out. Typically, the catalyst was etched hydrothermally in solution with pH value adjusted by H_2SO_4 to ∼2 for varied periods of time. After the etching process, p-nitrobenzoic acid was added into the system with the previously added H_2SO_4, and the following hydrogenation reaction was then carried out. The results are shown as entries 9−14. It is very impressive that the catalyst possesses unchanged catalytic activity, even after being etched for as long as 48 h. Moreover, the recyclability of the catalyst has been tested under a pH value of ∼2, and the activity can be maintained after 20 uses. The good durability of the catalyst under the harsh conditions demonstrates the unconventional robustness of the active sites on $CN/Ni/Al_2O_3$, which is particularly interesting. In addition, the catalyst shows
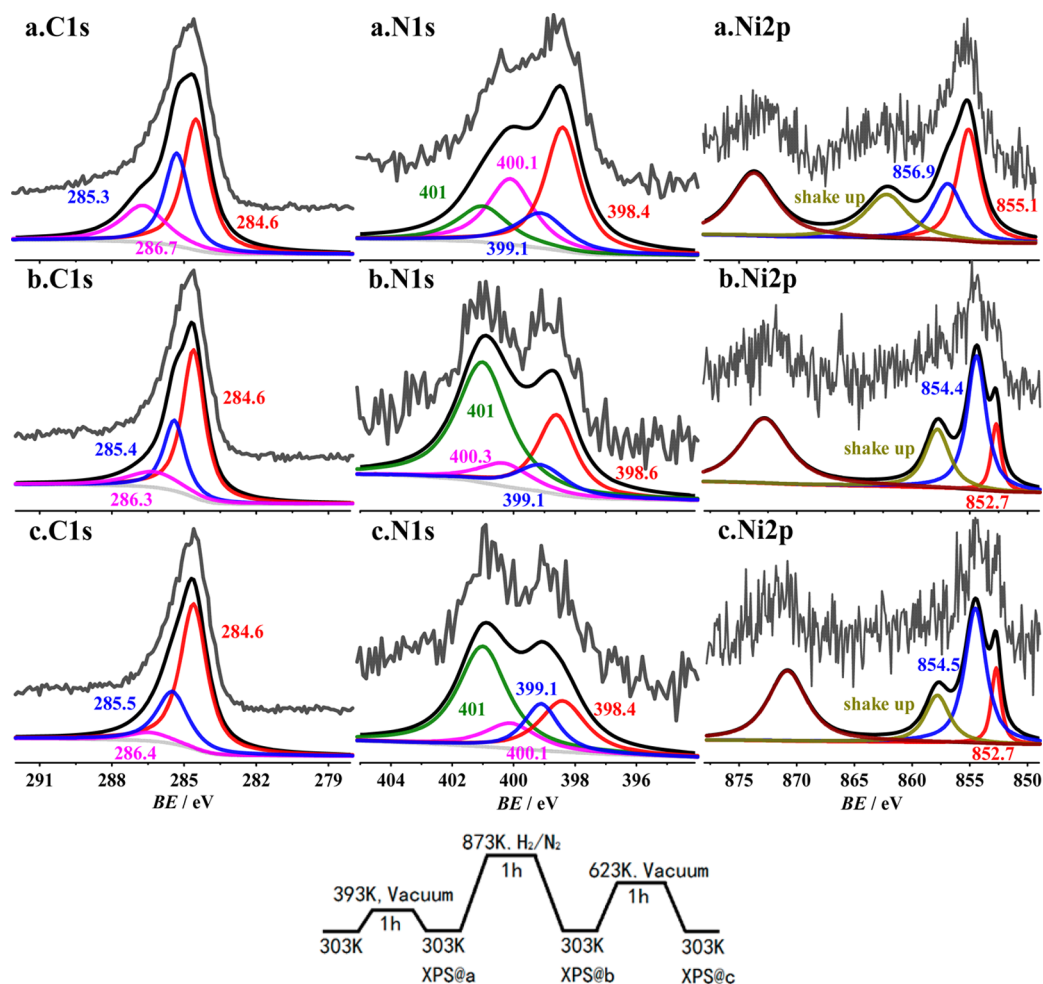

Figure 1. (a) TEM image of Al_2O_3 and (b) HRTEM image of $CN/Ni/Al_2O_3$.

Figure 2. XPS spectra recorded with the sample CN/Ni/Al$_2$O$_3$ experienced in situ treatment in a chamber connected directly to the apparatus, and the zigzag depicts the treatment procedure. (The gray lines in the spectra give the original data.)

good activity in the hydrogenation of 3-nitrobenzenesulfonic acid and the one-step hydrogenation of nitrobenzene to 4-amniophenol under strongly acidic conditions. More reaction data are shown in Table S1 (Supporting Information).
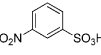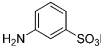
To reveal the details of this catalyst, various characterizations were conducted. In situ XPS results of CN/Ni/Al$_2$O$_3$ are shown in Figure 2, with the sample carefully treated in a chamber connected directly to the XPS system. After the sample was treated in vacuum at 393 K to remove the volatile impurities weakly adsorbed on the samples, the C 1s core level spectrum revealed the appearance of two additional carbon components to the typical sp^2-hybridized graphitic carbon (C^1) at 284.6 eV. The peak at 285.3 eV is attributed to the carbon atoms covalently bonded with nitrogen atoms in an aromatic structure (C^2), and the peak at 286.7 eV is attributed to the sp^2 hybridized carbon bonded to the −NH$_2$ group in the aromatic ring (C^3). The N 1s core level spectra can be deconvoluted into four peaks located at 398.4, 399.1, 400.1, and 401 eV, which can be assigned to the pyridinic nitrogen (N^1), the amine nitrogen (N^2), the pyrrol nitrogen (N^3), and the graphitic nitrogen (N^4), respectively (Figure 2).[31,32]

The Ni 2p$_{3/2}$ core level spectra can be divided into two peaks located at 855.1 and 856.9 eV, which is usually assign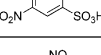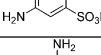ed to the oxidized nickel species.[33−38] Because the nickel is loaded on alumina and underneath CN, a relatively strong interaction could exist among the nickel, CN, and alumina, causing the

nickel to be in an electron-deficient metal state. The formation of Ni$_3$C could be excluded because of the different binding energy of nickel between Ni$_3$C and the nickel in the catalyst. There have been reports that the binding energy of the nickel on alumina increases to 856 eV as a result of a strong interaction with the alumina support;[39] nickel in Ni−Ru alloy transfers electrons to ruthenium and, hence, results in a higher binding energy of 853.1 eV.[40] Moreover, the nickel in Ni$_3$C has a binding energy of 853.5 eV due to the electron transfer from nickel to carbon.[41−46] Because the TEM image shows the (111) planes of nickel, it could be speculated that the nickel is in an electron-deficient state. The analysis results of the XPS measurement are summarized in Table 2.

After the catalyst was treated in 5 vol % H$_2$/N$_2$ at 873 K and cooled to 303 K in the H$_2$/N$_2$ with adsorption of H$_2$, some of nitrogen species in the sample had been lost as a result of the treatment at high temperature in hydrogen (SI Table S2). The metallic nickel (Ni^3) was then observed at 852.7 eV, and the additional species with binding energy of 854.4 eV were assigned to the surface nickel that had interacted strongly with CN (Ni^4). The following annealing treatment in vacuum at 623 K to remove adsorbed hydrogen causes the core level spectra of the three elements slightly changed. The adsorption of hydrogen has subtle influence on the electronic state of the three elements, which are in large quantity when compared with the adsorbed hydrogen species.

Table 1. Catalytic Performance of the Catalysts for Hydrogenation of Nitro Compounds to Amido Compounds under a Series of Conditions

Entry	Catalyst	pH	substrate	product	Conv. (%)	Sel.[*1] (%)
1[*2]	Ni/Al$_2$O$_3$	3.6			~100	100
2	Ni/Al$_2$O$_3$	~2			~0	--
3	CN/Al$_2$O$_3$	3.6			0	--
4	CN/Al$_2$O$_3$	~2			0	--
5	CN/Ni/Al$_2$O$_3$	3.6			82.8 / 100[*3]	100 / 100[*3]
6	CN/Ni/Al$_2$O$_3$	~3	(COOH / NO$_2$)	(COOH / NH$_2$)	72.4	100
7	CN/Ni/Al$_2$O$_3$	~2			79.2	100
8	CN/Ni/Al$_2$O$_3$	~1			83.4	100
9[*4]	CN/Ni/Al$_2$O$_3$	2, 2 h			79.3	100
10	CN/Ni/Al$_2$O$_3$	2, 8 h			82	100
11	CN/Ni/Al$_2$O$_3$	2, 12 h			85.7	100
12	CN/Ni/Al$_2$O$_3$	2, 24 h			80.0	100
13	CN/Ni/Al$_2$O$_3$	2, 36 h			82.4	100
14	CN/Ni/Al$_2$O$_3$	2, 48 h			83.4	100
15[*5]	Ni/Al$_2$O$_3$	~2	O$_2$N—...—SO$_3$H	H$_2$N—...—SO$_3$H	~0	--
16	CN/Ni/Al$_2$O$_3$	~2			100	100
17[*6]	CN/Ni/Al$_2$O$_3$	1.5 M H$_2$SO$_4$	(NO$_2$)	(NH$_2$ / OH)	80	100

[*1]The nitro compound reduced to the amino compound. [*2]Entries 1−8: cat., 50 mg; *p*-nitrobenzoic acid, 50 mg; mixed solution of methanol and water (4:1, v/v), 50 mL. Initial hydrogen pressure, 1 MPa; 393 K; 2 h. The pH value of the solution was 3.6 after *p*-nitrobenzoic acid was added. For the test under more acidic conditions, sulfuric acid was used to adjust the pH value of the solution. [*3]The reaction time was prolonged to 4 h. [*4]Entries 9−14 list the results of the etching test. Before the hydrogenation reaction, the catalyst was etched hydrothermally at 393 K in sulfuric acid (pH = 2) for different periods of time. After etching, the hydrogenation reaction was carried out under the same conditions as for entries 1−8. [*5]Entries 15 and 16: cat., 50 mg; 3-nitrobenzenesulfonic acid, 50 mg; 50 mL water. Initial hydrogen pressure: 1 MPa; 393 K; 2 h. [*6]Cat., 50 mg; nitrobenzene, 50 mg; 1.5 M H$_2$SO$_4$, 50 mL; CH$_3$OH, 1 mL. Initial hydrogen pressure, 1 MPa; 393 K; 2 h.

Table 2. Results of In Situ XPS Measurement on CN/Ni/Al$_2$O$_3$

treatment	C B.E. (eV)	species	area (%)	N B.E. (eV)	species	area (%)	Ni B.E. (eV)	species	area (%)
a	284.6	C^1	46	398.4	N^1	40	855.1	Ni^1	60
	285.3	C^2	31	399.1	N^2	17	856.9	Ni^2	40
	286.7	C^3	23	400.1	N^3	27			
				401	N^4	16			
b	284.6	C^1	58	398.6	N^1	26	852.7	Ni^3	20
	285.4	C^2	27	399.1	N^2	11	854.4	Ni^4	80
	286.3	C^3	15	400.3	N^3	10			
				401	N^4	53			
c	284.6	C^1	67	398.4	N^1	23	852.7	Ni^3	20
	285.5	C^2	26	399.1	N^2	15	854.5	Ni^4	80
	286.4	C^3	7	400.1	N^3	12			
				401	N^4	50			

*C^1, graphitic carbon; C^2, carbon neighboring graphitic nitrogen; C^3, carbon attached to the −NH$_2$ group. N^1, pyridinic nitrogen; N^2, amine nitrogen; N^3, pyrrol nitrogen; N^4, graphitic nitrogen. Ni^1 and Ni^2, oxidized nickel interacted with alumina; Ni^3, metallic nickel; Ni^4, metallic nickel strongly interacted with CN, donating electrons to the later. The treatment conditions of a, b, and c are the same as Figure 3.

The densities of state of valence bands (VB) of the CN/Al$_2$O$_3$ and CN/Ni/Al$_2$O$_3$ are measured to determine the effect of nickel doping on the VB edge of CN, as shown in Figure 3a. In contrast to CN/Al$_2$O$_3$, the CN/Ni/Al$_2$O$_3$ demonstrates a VB maximum upshift from 1.54 to 0.51 eV, indicating a possible electron transfer from metal to CN, the doping effect. The small structure near the Fermi level, fitted as a small peak, should be attributed to the electron states from nitrogen of CN.

Figure 3b depicts the variation of conduction of the samples with temperature around 423 K. The conductance of CN/Ni/Al$_2$O$_3$ is much better than CN/Al$_2$O$_3$, revealing the doping effect of nickel to CN, and the smaller activation energy of CN/Ni/Al$_2$O$_3$ also reflects its better conductance than CN/Al$_2$O$_3$. The conductions of the two samples in argon and hydrogen (Figure 3c) show the strong adsorption and doping effect of hydrogen on CN/Ni/Al$_2$O$_3$, whereas the conductance of CN/
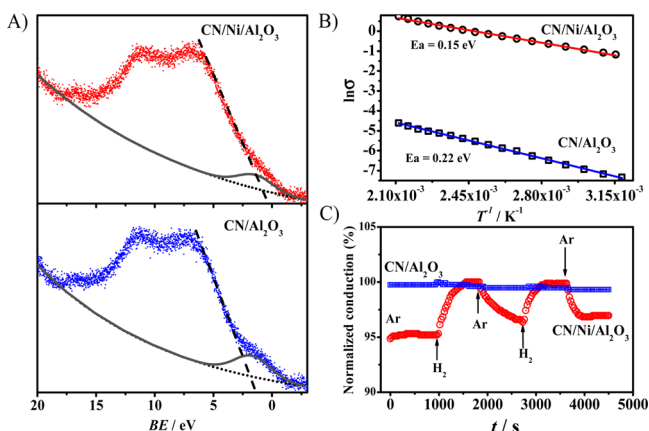
Figure 3. (A) The valence band spectra of CN/Ni/Al$_2$O$_3$ and CN/Al$_2$O$_3$ measured by XPS. The charging effect of the samples is neutralized with dispersive electrons of low energy. (B) The variation of conduction of the samples with temperature around 423 K. (C) The conduction of the samples in Ar and H$_2$.

Al$_2$O$_3$ is little affected by the atmosphere of argon or hydrogen, which is relatively inert for adsorption of hydrogen.

To detect the surface hydrogen qualitatively and quantitatively, the exchange of gaseous D$_2$ with the adsorbed hydrogen was carried out. Figure 4 displays the HD evolution with the increasing temperature of the samples. For Al$_2$O$_3$, the HD evolution peak, peak α, is observed at 645 K, mainly from the hydroxyls, that is, HO–Al. The Ni/Al$_2$O$_3$ shows mainly two evolution peaks at 410 and 457 K: the first peak, that is, the γ peak, is attributed to the chemisorbed hydrogen on the nickel; the second is due to the hydroxyls (α species) of the alumina support, which moves to lower temperatures by the catalysis of the nickel for the dissociation of H$_2$.[47−50] After the encapsulation of Al$_2$O$_3$ with CN, the peak temperature for H–D exchange is delayed to 765 K, reflecting the hydrogen tightly bonded to CN on Al$_2$O$_3$, that is, the δ species. Even when the sample was cooled in hydrogen, we could not detect any hydrogen adsorbed on the CN/Al$_2$O$_3$. For CN/Ni/Al$_2$O$_3$, however, a new peak for HD located at 516 K emerges, of which the exchange temperature is higher than that of hydrogen chemisorbed on Ni/Al$_2$O$_3$ but much lower than the hydrogen tightly bonded to CN/Al$_2$O$_3$. This demonstrates the hydrogen, ε species, adsorbed on the CN supported by nickel and exchanged with deuterium at temperatures higher than that for the hydrogen adsorbed directly on Ni, revealing that the activation of the chemisorbed hydrogen on CN/Ni/Al$_2$O$_3$ is inferior to those on Ni/Al$_2$O$_3$.

In situ FT-IR experiments are performed to further study the active sites for hydrogen adsorption of the catalyst, and the results are shown in Figure 4b. In the spectra of CN/Ni/Al$_2$O$_3$, a wide band between 3050 and 3790 cm^{-1} has emerged after treatment in hydrogen. This band should be assigned to the vibration of N–H similar bonds. This suggests that the surface nitrogen is the site for hydrogen chemisorption. The wide range of this band demonstrates the distribution of the electronic environment of the surface nitrogen. After the H–D exchange, the $\nu_{(N-H)}$ band between 3450−3790 cm^{-1} disappeared and a new wide band around 2650 cm^{-1} emerged. This band should be assigned to the N-D vibration[51−53] and is related by the $1/\sqrt{2}$ factor with the corresponding frequency value of the $\nu_{(N-H)}$ band. This is the H/D isotopic effect found in the IR spectroscopy of bonded hydrogen.[53−55] After
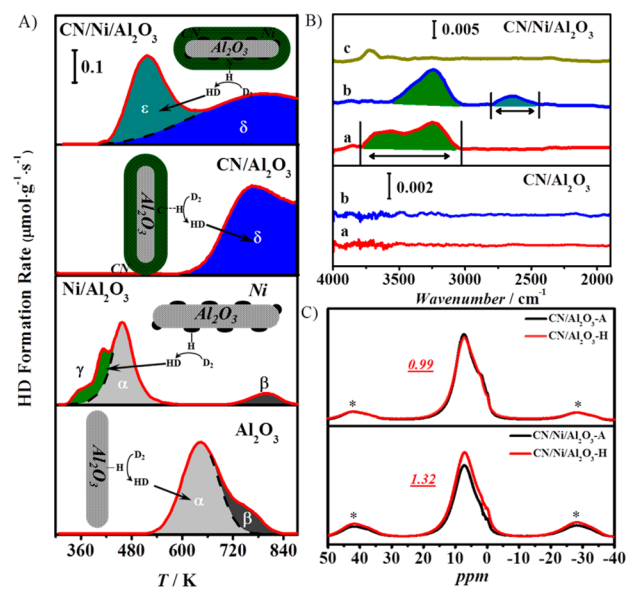

Figure 4. (A) H−D exchange profiles of the samples; red lines are the experimental data. The sample was pretreated in 5 vol % H$_2$/N$_2$ at 873 K for 1 h and cooled in the same atmosphere, for adsorption of H$_2$, to room temperature and switched to Ar to remove the physically adsorbed H$_2$. The sample was then heated in 5 vol % D$_2$/Ar, during which the signal of HD was monitored by mass spectrometry. (B) FT-IR spectra of CN/Ni/Al$_2$O$_3$ and CN/Al$_2$O$_3$ measured in an in situ cell: (a) with hydrogen adsorption, (b) after partial exchange of D$_2$ with the adsorbed H$_2$, and (c) the sample treated in vacuum at 623 K to remove the chemisorbed hydrogen. (C) ^{1}H NMR spectra of CN/Ni/Al$_2$O$_3$ and CN/Al$_2$O$_3$ with (H) or without (A) hydrogen adsorption. The underlined italic number shows the ratio of the relative peak area after and before hydrogen adsorption. For the measurement shown in the figure, a ^{1}H Hahn-echo sequence was used with a π/2 pulse of 2.3 μs width, and the spinning speed was 14 000 Hz. For CN/Al$_2$O$_3$ and CN/Ni/Al$_2$O$_3$, a total of 256 scans and 2048 scans were collected with recycle delays of 4 and 0.5 s, respectively. Asterisks (*) in these spectra denote spinning sidebands. (For the IR and NMR measurement, the sample treatment referenced to the H−D exchange.)

evacuation of the system at 623 K to desorb hydrogen, the $\nu_{(N-H)}$ band between 3050 and 3790 cm^{-1} vanishes.

For CN/Al$_2$O$_3$, the FT-IR spectra stays nearly the same after hydrogen treatment, suggesting that the CN is not capable of adsorbing hydrogen without the contribution of nickel. The FTIR spectra provide direct evidence that the nickel-modified CN is capable of adsorbing and activating hydrogen and formed a chemical bond similar to the N−H bonds with the nitrogen in CN matrix, making this amine-like group responsible for the reduction of the −NO$_2$ group under acidic conditions. The hydrogen species adsorbed by the samples are double-checked by ^{1}H NMR, as shown in Figure 4c. The results prove again that the sample CN/Ni/Al$_2$O$_3$ is capable of adsorption of hydrogen. Unfortunately, the relation of the chemisorbed hydrogen with the nitrogen species in CN is actually not given with current NMR measurement because of the too-low content of ^{15}N isotope in the samples.

Summing up the above-mentioned results, Figure 5 shows the mechanism diagram of the high-performance catalyst composed of CN covered on nickel for hydrogenation reactions under harsh conditions. The nickel donates electrons to the CN and gives the latter the ability to adsorb and activate hydrogen, which functions to reduce nitro groups in organic molecules to amino groups with high selectivity, even under strongly acidic
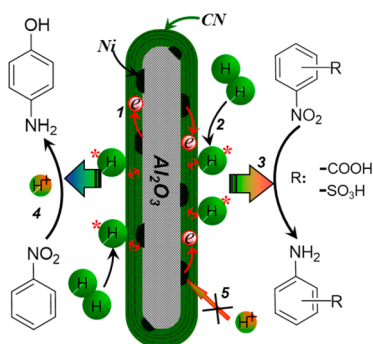
Figure 5. Schematic of the principle of the mesostructural CN catalyst with underlying nickel. The points are (1) electron donation from nickel to CN; (2) dissociative adsorption of the hydrogen molecule bonded to the CN; (3) reduction of the nitro compound by the activated hydrogen; (4) the adsorbed hydrogen is capable of hydrogenation under strong acidic conditions, with concentrated protons taking part in the reaction for the rearrangement of the intermediate; and (5) nickel is protected from corrosion or poisoning.

conditions. Meanwhile, the nickel is protected from corrosion or poisoning by the encapsulating robust CN layer. The hydrogen species adsorbed by the new active sites of CN with underlying nickel on alumina demonstrated here provide us more design thoughts for new catalysts, in addition to its high stability under harsh conditions. It must be also valuable for other important reactions, such as the selective hydrogenation of acetylene to ethene.[56,57] Continued work is in progress.

3. CONCLUSION

In conclusion, by encapsulating highly dispersed nickel on alumina with CN, we have demonstrated a successful tuning of the electronic properties of CN, which provides it with the ability to adsorb and activate hydrogen for reaction with nitro compounds to amino compounds. The metallic nickel donates electrons to CN, with which the surface nitrogen atoms, showing a relatively independent state of electron enrichment, offer the sites for hydrogen adsorption and activation. At the same time, direct contact of the metal with the harsh environment is avoided. The catalyst is highly stable and active for the hydrogenation of nitro compounds under acidic conditions and also shows high performance for the one-step synthesis of *p*-amoniophenol with hydrogenation of nitrobenzene in 15 wt % sulfuric acid. The current report demonstrates a novel concept, noncontact tuning of the catalyst, using CN material to develop efficient catalysts for practical reactions and offers a powerful tool to the chemical industry.

4. EXPERIMENTAL SECTION

Preparation of Al_2O_3 and NiO/Al_2O_3. Al_2O_3 was prepared by the following method: In a typical synthesis, alumina sol was prepared by the controlled hydrolysis of aluminum isopropoxide. Next, the alumina sol (18 g) was added to the mixture of oleylamine (1.4 g, Adrich) and $NH_3 \cdot H_2O$ (1 mL, 25%) in 15 mL distilled water at 353 K, and the mixture was kept at 353 K for another 2 h. The resultant was transferred into the autoclave and then was sealed and kept at 453 K for 72 h. After hydrothermal treatment, the powder was filtered, washed with ethanol, and then dried at 373 K. Finally, the powder was calcined at 823 K in air for 4 h to obtain the Al_2O_3. The NiO/Al_2O_3 samples were prepared by an impregnation method, and

$Ni(NO_3)_2 \cdot H_2O$ was used as a metallic salt precursor for the preparation of NiO. In this article, we synthesized NiO/Al_2O_3 with a loading of 4 wt %. Typically, $Ni(NO_3)_2$ solution (0.5 mL, 1.4 M) was added into Al_2O_3 (1 g). The resulting sample was dried at 393 K for 12 h and then calcined at 723 K for 4 h to obtain NiO/Al_2O_3.

Encapsulation of NiO/Al_2O_3 with CN. In a typical synthesis, NiO/Al_2O_3 (1 g) was added to *m*-xylene (80 mL), then ethylenediamine (2 g) and carbon tetrachloride (4 g) were added to the system. After that, the system was first heated to 363 K and stirred for 4 h and then heated to 413 K and stirred for another 4 h. The resulting dark brown solid mixture was placed in the drying oven for 12 h and ground into a fine powder. The composite was treated in a nitrogen flow of 50 mL·min⁻¹ at 873 K at a heating rate of 2 K·min⁻¹ and kept at these conditions for 6 h to carbonize the polymer. The product was labeled as $CN/Ni/Al_2O_3$.

Characterization. X-ray diffraction (XRD) patterns were taken on a Phillips X'Pro diffractometer using Cu Kα radiation (λ = 1.5418 Å) at 40 kV and 25 mA. Fourier transform infrared spectra (FT-IR) for the samples were collected on a Bruker Vertex 70 spectrophotometer using KBr pellets, recording at 64 scans with a resolution of 4 cm⁻¹. Transmission electron microscopy (TEM) measurements were conducted using a JEOL JEM-200CX instrument at an accelerating voltage of 200 kV. Thermogravimetric curves were taken on a STA 449C-Thermal Star 300 instrument (Netzsch, Germany) in air atmosphere with a heating rate of 10 K·min⁻¹ to 1073 K.

D/H exchange: The catalyst sample (200 mg) was reduced in 5 vol % H_2/N_2 (30 mL·min⁻¹) at a heating rate of 10 K·min⁻¹ to 873 K and kept at this temperature for 1 h. Then the sample was cooled in the same atmosphere to room temperature, for adsorption of H_2, and switched to Ar (35 mL·min⁻¹) to remove the physically adsorbed H_2. Deuterium exchanged with protonium presented in the sample was measured by increasing the temperature to 873 K at a heating rate of 10 K·min⁻¹. The signal of HD was monitored by mass spectrometry.

X-ray photoelectron spectroscopy (XPS): The XPS measurements were performed in a commercial XPS system (PHI 5000 VersaProbe) equipped with a hemispherical electron analyzer and monochromatic Al Kα X-ray exciting source. The sample was first evacuated at 393 K for 1 h, then cooled to room temperature, and the spectra were measured. Then the sample was reduced at 873 K in a 5 vol % H_2/N_2 (30 mL·min⁻¹) for 1 h. After the sample was cooled to room temperature, the spectra were measured. Finally, the sample was heated to 623 K in vacuum for 1 h, and the spectra were measured at room temperature.

In situ FT-IR: The experiment was performed on a Bruker Tensor 27 spectrophotometer. The catalysts were compressed to obtain disks and then installed in an in situ absorption cell. The samples were first activated at 673 K in Ar (35 mL·min⁻¹) for 1 h. After being cooled to room temperature, the spectrum was recorded as background. The hydrogen adsorption of the samples was performed in 5 vol % H_2/Ar (50 mL·min⁻¹) at 423 K for 30 min, then after the samples were cooled to room temperature, the spectrum was recorded. Then two different measurements were taken independently: (1) Deuterium exchanged with protonium presented in the sample was carried out by increasing the temperature to 453 K in 5 vol % D_2/Ar (30 mL·min⁻¹) and keeping it at this temperature for 1 h. After the sample was cooled to room temperature, the spectrum was

recorded. (2) The samples were evacuated to 10^{-3} Torr at room temperature for 2 h, and the spectrum was recorded afterward.

Conductance measurement: The conductance of the catalysts was determined by measuring the specific resistance of sample disc with the two-electrode DC method. The sample was compacted into a disc (nearly 2 mm thick and 13 mm diameter) with two electrodes; each was made by spot-welding to silver leads (0.1 mm diameter) with conductive silver paste. The final disc was further heated at 873 K for 1 h, and the conduction of the samples was measured at different temperatures in Ar to determine the activation energy of conduction. Then the samples were kept at 423 K, and the conduction in different atmospheres was measured by switching the gas flow between Ar and H_2.

Solid state nuclear magnetic resonance: ^1H MAS NMR spectra were obtained from a Bruker Avance III spectrometer with a 89 mm wide-bore 9.4 T superconducting magnet in a 4 mm rotor at 400.1 MHz. ^1H chemical shifts are referenced to adamantine (1.78 ppm). The sample (0.2 g) was first activated at 673 K in Ar (35 mL·min^{-1}) for 1 h, then part of the sample (0.1 g) was taken out to obtain the spectra. The rest of the sample was treated at 423 K in 5 vol % H_2/Ar (50 mL·min^{-1}) for 30 min, and the spectra were obtained afterward. All the sample treatment was carried out in a glovebox.

Catalytic Test. The hydrogenation reaction was carried out in a bath-type autoclave reactor. In a typical reaction, catalyst (50 mg) and p-nitrobenzoic acid or other molecules (50 mg) were added into the mixed solvent of CH_3OH/H_2O (4:1 vol, 50 mL). The pH value was adjusted by adding H_2SO_4 solution into the system. Hydrogen was introduced into the reactor at room temperature to a pressure of 1.0 MPa. The reactor was then heated to 393 K and kept at this temperature for 2 h. After the reaction, the reactor was cooled to room temperature naturally, and the catalyst was filtered. The resulting solution was analyzed by HPLC. The Agilent HPLC 2016 was equipped with a C18 column and an UV detector (254 nm). The eluent was methanol/0.02 M ammonium acetate solution (65/35).

ASSOCIATED CONTENT

Ⓢ Supporting Information

XRD patterns of the samples; IR spectra and TG profiles of CN/Al_2O_3 and $CN/Ni/Al_2O_3$; surface compositions of the catalysts measured by XPS; more reaction data obtained on a series samples, including $CN/Co/Al_2O_3$, $CN/Cu/Al_2O_3$, and $CN/Fe/Al_2O_3$, etc.; catalytic performances of $CN/Ni/Al_2O_3$ with different contents of nickel. This material is available free of charge via the Internet at http://pubs.acs.org.

AUTHOR INFORMATION

Corresponding Author

*Phone: +86 25 83595077. Fax: +86 25 83686251. E-mail: dingwp@nju.edu.cn.

Notes

The authors declare no competing financial interest.

ACKNOWLEDGMENTS

REFERENCES

(1) Komatsu, T.; Hirose, T. *Appl. Catal., A* **2004**, *276*, 95−102.
(2) Tanielyan, S. K.; Nair, J. J.; Marin, N.; Alvez, G.; McNair, R. J.; Wang, D.; Augustine, R. L. *Org. Process Res. Dev.* **2007**, *11*, 681−688.
(3) Wang, S.; Ma, Y.; Wang, Y.; Xue, W.; Zhao, X. *J. Chem. Technol. Biotechnol.* **2008**, *83*, 1466−1471.
(4) Nadgeri, J. M.; Biradar, N. S.; Patil, P. B.; Jadkar, S. T.; Garade, A. C.; Rode, C. V. *Ind. Eng. Chem. Res.* **2011**, *50*, 5478−5484.
(5) Wang, S.; He, B.; Wang, Y.; Zhao, X. *Catal. Commun.* **2012**, *24*, 109−113.
(6) Liu, A. Y.; Cohen, M. L. *Science* **1989**, *245*, 841−842.
(7) Kaner, R. B.; Gilman, J. J.; Tolbert, S. H. *Science* **2005**, *308*, 1268−1269.
(8) Lee, J. S.; Wang, X.; Luo, H.; Baker, G. A.; Dai, S. *J. Am. Chem. Soc.* **2009**, *131*, 4596−4597.
(9) Wang, E. G. *Prog. Mater. Sci.* **1997**, *41*, 241−298.
(10) Wang, Y.; Wang, X.; Antonietti, M. *Angew. Chem., Int. Ed.* **2012**, *51*, 68−89.
(11) Teter, D. M.; Hemley, R. J. *Science* **1996**, *271*, 53−55.
(12) Jin, X.; Balasubramanian, V. V.; Selvan, S. T.; Sawant, D. P.; Chari, M. A.; Lu, G. Q.; Vinu, A. *Angew. Chem., Int. Ed.* **2009**, *48*, 7884−7887.
(13) Wang, Q. H.; Jin, Z.; Kim, K. K.; Hilmer, A. J.; Paulus, G. L. C.; Shih, C.-J.; Ham, M.-H.; Sanchez-Yamagishi, J. D.; Watanabe, K.; Taniguchi, T.; Kong, J.; Jarillo-Herrero, P.; Strano, M. S. *Nat. Chem.* **2012**, *4*, 724−732.
(14) Zhang, J.; Zhang, M.; Sun, R. Q.; Wang, X. *Angew. Chem., Int. Ed.* **2012**, *51*, 10145−10149.
(15) Wang, X.; Maeda, K.; Thomas, A.; Takanabe, K.; Xin, G.; Carlsson, J. M.; Domen, K.; Antonietti, M. *Nat. Mater.* **2009**, *8*, 76−80.
(16) Zhang, J.; Grzelczak, M.; Hou, Y.; Maeda, K.; Domen, K.; Fu, X.; Antonietti, M.; Wang, X. *Chem. Sci.* **2012**, *3*, 443−446.
(17) Cui, Y.; Huang, J.; Fu, X.; Wang, X. *Catal. Sci. Technol.* **2012**, *2*, 1396−1402.
(18) Zhang, J.; Chen, X.; Takanabe, K.; Maeda, K.; Domen, K.; Epping, J. D.; Fu, X.; Antonietti, M.; Wang, X. *Angew. Chem., Int. Ed.* **2010**, *49*, 441−444.
(19) Wang, X.; Maeda, K.; Chen, X.; Takanabe, K.; Domen, K.; Hou, Y.; Fu, X.; Antonietti, M. *J. Am. Chem. Soc.* **2009**, *131*, 1680−1681.
(20) Zheng, Y.; Jiao, Y.; Chen, J.; Liu, J.; Liang, J.; Du, A.; Zhang, W.; Zhu, Z.; Smith, S. C.; Jaroniec, M.; Lu, G. Q.; Qiao, S. Z. *J. Am. Chem. Soc.* **2011**, *133*, 20116−20119.
(21) Czerw, R.; Terrones, M.; Charlier, J. C.; Blase, X.; Foley, B.; Kamalakaran, R.; Grobert, N.; Terrones, H.; Tekleab, D.; Ajayan, P. M.; Blau, W.; Rühle, M.; Carroll, D. L. *Nano Lett.* **2001**, *1*, 457−460.
(22) Carvalho, A. C. M.; dos Santos, M. C. *J. Appl. Phys.* **2006**, *100*, 084305.
(23) Wang, Y.; Yao, J.; Li, H.; Su, D.; Antonietti, M. *J. Am. Chem. Soc.* **2011**, *133*, 2362−2365.
(24) Datta, K. K.; Reddy, B. V.; Ariga, K.; Vinu, A. *Angew. Chem., Int. Ed.* **2010**, *49*, 5961−5965.
(25) Xu, X.; Li, Y.; Gong, Y.; Zhang, P.; Li, H.; Wang, Y. *J. Am. Chem. Soc.* **2012**, *134*, 16987−16990.
(26) Zhang, P.; Yuan, J.; Fellinger, T.-P.; Antonietti, M.; Li, H.; Wang, Y. *Angew. Chem., Int. Ed.* **2013**, *52*, 6028−6032.
(27) Zhang, P.; Gong, Y.; Li, H.; Chen, Z.; Wang, Y. *Nat. Commun.* **2013**, *4*, 1593−1604.
(28) Di, Y.; Wang, X.; Thomas, A.; Antonietti, M. *ChemCatChem* **2010**, *2*, 834−838.
(29) Qiu, Y.; Gao, L. *Chem. Commun.* **2003**, 2378−2379.
(30) Wang, X.; Chen, X.; Thomas, A.; Fu, X.; Antonietti, M. *Adv. Mater.* **2009**, *21*, 1609−1612.
(31) Hellgren, N.; Guo, J.; Luo, Y.; Såthe, C.; Agui, A.; Kashtanov, S.; Nordgren, J.; Ågren, H.; Sundgren, J.-E. *Thin Solid Films* **2005**, *471*, 19−34.
(32) Arrigo, R.; Havecker, M.; Schlogl, R.; Su, D. S. *Chem. Commun.* **2008**, 4891−4893.
(33) Grosvenor, A. P.; Biesinger, M. C.; Smart, R. S. C.; McIntyre, N. S. *Surf. Sci.* **2006**, *600*, 1771−1779.

(34) Kovács, G. J.; Bertóti, I.; Radnóczi, G. *Thin Solid Films* **2008**, *516*, 7942−7946.

(35) Abrasonis, G.; Scheinost, A. C.; Zhou, S.; Torres, R.; Gago, R.; Jiménez, I.; Kuepper, K.; Potzger, K.; Krause, M.; Kolitsch, A.; Möller, W.; Bartkowski, S.; Neumann, M.; Gareev, R. R. *J. Phys. Chem. C* **2008**, *112*, 12628−12637.

(36) Nesbitt, H. W.; Legrand, D.; Bancroft, G. M. *Phys. Chem. Min.* **2000**, *27*, 357−366.

(37) Wanger, C. D.; Riggs, W. M.; Davis, L. E.; Davis, L. E.; Moulder, J. F.; Mülenberg, G. E. *Handbook of X-Ray Photoelectron Spectroscopy*; Perkin-Elmer: Muilenberg, Germany, 1979.

(38) Benchikh, N.; Garrelie, F.; Donnet, C.; Bouchet-Fabre, B.; Wolski, K.; Rogemond, F.; Loir, A. S.; Subtil, J. L. *Thin Solid Films* **2005**, *482*, 287−292.

(39) Feng, J. T.; Lin, Y. J.; Evans, D. G.; Duan, X.; Li, D. Q. *J. Catal.* **2009**, *266*, 351−358.

(40) Zhao, Z. F.; Wu, Z. J.; Zhou, L. X.; Zhang, M. H.; Li, W.; Tao, K. Y. *Catal. Commun.* **2008**, *9*, 2191−2194.

(41) Hong, N.; Langell, M. A.; Liu, J.; Kizilkaya, O.; Adenwalla, S. *J. Appl. Phys.* **2010**, *107*, 024513.

(42) Juan Matos, M. R.; González, G.; de Navarro, C. U. *Open Mater. Sci. J.* **2010**, *4*, 125−132.

(43) Wiltner, A.; Linsmeier, C. *Phys. Status Solidi A* **2004**, *201*, 881−887.

(44) Czekaj, I.; Loviat, F.; Raimondi, F.; Wambach, J.; Biollaz, S.; Wokaun, A. *Appl. Catal., A* **2007**, *329*, 68−78.

(45) Goto, Y.; Taniguchi, K.; Omata, T.; Otsuka-Yao-Matsuo, S.; Ohashi, N.; Ueda, S.; Yoshikawa, H.; Yamashita, Y.; Oohashi, H.; Kobayashi, K. *Chem. Mater.* **2008**, *20*, 4156−4160.

(46) El Mel, A. A.; Bouts, N.; Grigore, E.; Gautron, E.; Granier, A.; Angleraud, B.; Tessier, P. Y. *J. Appl. Phys.* **2012**, *111*, 114309.

(47) Almasan, V.; Gaeumann, T.; Lazar, M.; Marginean, P.; Aldea, N. *Stud. Surf. Sci. Catal.* **1997**, *109*, 547−552.

(48) Almasan, V.; Lazar, M.; Marginean, P. *Stud. Surf. Sci. Catal.* **1999**, *122*, 435−438.

(49) Thomas, C.; Vivier, L.; Travert, A.; Maugé, F.; Kasztelan, S.; Pérot, G. *J. Catal.* **1998**, *179*, 495−502.

(50) Marginean, P.; Olariu, A. *Appl. Catal., A* **1997**, *165*, 241−248.

(51) Flakus, H. T.; Michta, A.; Nowak, M.; Kusz, J. *J. Phys. Chem. A* **2011**, *115*, 4202−4213.

(52) Issaoui, N. *Open J. Phys. Chem.* **2012**, *02*, 228−239.

(53) Flakus, H. T.; Hachula, B.; Stolarczyk, A. *Spectrochim. Acta, Part A* **2012**, *85*, 7−16.

(54) Pimentel, G. C.; McClellan, A. L. *The Hydrogen Bond*; W. H. Freeman: San Francisco, 1976.

(55) *The Hydrogen Bond: Recent Developments in the Theory and Experiment, Parts I, II and III*; Schuster, P.; Zundel, G.; Sandorfy, C., Eds.; Elsevier: Amsterdam, 1976.

(56) Armbrüster, M.; Kovnir, K.; Friedrich, M.; Teschner, D.; Wowsnick, G.; Hahne, M.; Gille, P.; Szentmiklósi, L.; Feuerbacher, M.; Heggen, M.; Girgsdies, F.; Rosenthal, D.; Schlögl, R.; Grin, Y. *Nat. Mater.* **2012**, *11*, 690−693.

(57) Studt, F.; Abild-Pedersen, F.; Bligaard, T.; Sørensen, R. Z.; Christensen, C. H.; Nørskov, J. K. *Science* **2008**, *320*, 1320−1322.